

# Profiling Active Compounds from Citrus and Mangosteen Peels as Excellent Antiviral Agents Using an In-Silico Study Approach

Nurul Jadid Mubarakati<sup>1</sup>, Honesty Nurizza Pinanti<sup>1</sup>, Sama' Iradat Tito<sup>2</sup>

<sup>1</sup>Department of Biology, Universitas Negeri Surabaya, Surabaya 60231, Indonesia

<sup>2</sup>Department of Biology, Universitas Islam Malang, Malang 65144, Indonesia

**Abstract.** SARS-CoV-2 remains a global health concern, with active cases and new variants still reported in mid-2025, especially among vulnerable groups with comorbidities. Orange and mangosteen peels contain bioactive compounds, such as flavonoids and xanthenes, with potential antiviral activity. This study aimed to analyze and predict their pharmacokinetic, toxicity, and binding-affinity properties as antiviral agents using an *in silico* approach through ADMET-toxicity screening via pkCSM and molecular docking. Twenty-five compounds were tested as ligands, along with one native ligand as a positive control. Seven active compounds from both peels met criteria for good oral drug candidates and were suitable for further docking analysis. All showed stronger binding affinity than the positive control. Orange-peel compounds such as Valencene,  $\alpha$ -Phellandrene,  $\alpha$ -Terpinol, and  $\alpha$ -Copaene could disrupt RBD–ACE2 interactions, while Valencene and Cadinene may inhibit RBD allosterically. Mangosteen-peel compounds—including Smeathxanthone A, Garcinone B, Mangostenon A, Tovophyllin B, and Anthocyanins—also demonstrated potential allosteric inhibition. These findings highlight citrus and mangosteen peels as promising natural antiviral sources. Further *in vitro* and *in vivo* studies are required to validate these results and explore structural refinement of the most potent compounds.

**Keywords:** antiviral, compound, citrus peel, *in silico*, mangosteen peel.

## 1 Introduction

COVID-19, caused by a newly emerged coronavirus, was declared a global pandemic on March 11, 2020. WHO reported over 196 million cases and 4.2 million deaths in 2021. While most patients experience mild symptoms, older adults and individuals with comorbidities face a higher risk of severe illness. Despite declining transmission, SARS-CoV-2 persists, with approximately 147,000 new cases and 4,500 deaths still reported worldwide between 6 January and 2 February 2025. The Ministry of Health recommends antivirals such as Paxlovid, Molnupiravir, and Remdesivir, although their high cost and side effects limit wider

---

<sup>1</sup> Corresponding author: [nurulmubarakati@unesa.ac.id](mailto:nurulmubarakati@unesa.ac.id)

use [1]. Consequently, natural product-based antivirals are increasingly explored, especially given Indonesia's biodiversity. A zero-waste approach to medicinal plants enhances sustainability, and citrus and mangosteen peels—abundant agricultural by-products—are promising sources of bioactive compounds with potential activity against SARS-CoV-2.

Some of the plants that grow in tropical or subtropical areas and are believed to possess antiviral activities are orange and mangosteen. Beyond the fruits, the peels of orange and mangosteen contain numerous bioactive compounds whose potential benefits have yet to be fully optimized. Based on previous studies, orange peel has main components, including flavonoid derivative compounds (Naringenin, hesperetin, flavones and their derivatives), while mangosteen peel contains active compounds from the xanthenes group (Mangostin, Alpha Mangostin, Beta Mangostin, Mangostenol, Mangostanol, Mangostinon A, Mangostenon B, Tovophyllin B, Trapezifolixanthone, Garcinon B, Flavonoid Epicatechin, and Gartanin) [2]. Several studies have shown that orange peel and mangosteen have a million bioactivities, including antiviral properties. In orange peel, flavonoid derivative compounds were chosen as inhibitors because they have been proven to be antiviral [3]. Naringenin and hesperetin, classified as flavonoids, have been studied as inhibitors for the COVID-19 virus [4]. Flavones and their derivatives have been studied and used as influenza virus inhibitors [5]. Moreover, the mangosteen peel contains compounds that have pharmacological activity, including anti-inflammatory, antihistamine, antibacterial, antifungal, antimalarial, hypertension, stroke, HIV therapy, and anti-aging effects [6]. As an antimicrobial agent, the ability of xanthenes has been tested by [6], who reported that the administration of 6.25 µg/mL of xanthone derivatives, such as alpha-mangostin, beta-mangostin, and B-garcinone, can inhibit tuberculosis bacteria. However, the identification of active compounds in orange and mangosteen peels and their potential for antivirals in combating COVID-19 through an *in silico* approach has not been widely carried out.

The causative agent of COVID-19 is severe acute respiratory syndrome coronavirus 2 (SARS-CoV-2). The virus infection is primarily mediated by the interaction between the receptor-binding domain (RBD) of the viral S1 glycoprotein and the angiotensin-converting enzyme 2 (ACE2) receptor on its host cells [7]. The binding of RBD to ACE2 facilitates the virus to penetrate and subsequently replicate within host cells. The virus invades the lower respiratory tract by invading lung epithelial cells, delivering its nucleocapsid, and hijacking the host cellular machinery for replication in the cytoplasm [8]. Moreover, the virus infection can lead to organ damage and multi-organ failure, impacting vital systems such as the heart, kidneys, liver, central nervous system, and gastrointestinal tract [9]. Therefore, targeting the RBD of the S1 glycoprotein becomes a promising strategy in inhibiting the viral infection. This study aims to identify the potential of active compounds in orange and mangosteen peels as effective antiviral agents in combating COVID-19, particularly by targeting the wild-type RBD structure through an *in silico* approach.

This study serves as an important preliminary step prior to *in-vitro* and *in-vivo* testing. Although mutations in the RBD continue to emerge, the wild-type RBD structure remains a relevant model for understanding the fundamental interactions between the virus and its host cells. The novelty of this research lies in its *in-silico* evaluation of bioactive compounds specifically derived from citrus and mangosteen peels—natural by-products that have been largely underexplored as antiviral candidates against SARS-CoV-2. Unlike previous studies that generally focus on single phytochemicals or well-known plant metabolites, this study integrates a zero-waste concept with molecular docking on the wild-type RBD to identify potential inhibitors from underutilized resources. This approach provides new insights into conserved binding residues and offers a sustainable foundation for future investigations involving mutated RBD structures.

## **2 Materials and methods**

The materials used in this study included 2-acetamido-2-deoxy- $\beta$ -D-glucopyranose as the native ligand and 25 bioactive compounds derived from orange and mangosteen peels. The receptor structure employed for molecular docking was the SARS-CoV-2 RBD crystal structure (PDB ID: 7BZ5), obtained from the Protein Data Bank. Several software tools were utilized, including PyRx, BIOVIA Discovery Studio, PubChem, and the pkCSM online platform. Pharmacokinetic and toxicity assessments were conducted using pkCSM by entering the SMILES codes of each compound. All applications required for the analysis were installed in the biocomputing laboratory following applicable safety procedures. Ligand structures were downloaded from PubChem in SDF format and converted to PDB format using Chimera 1.4. The 7BZ5 receptor was prepared by removing unnecessary ligands, chains, and water molecules prior to docking. Molecular docking was performed in PyRx by importing the prepared receptor and ligands, defining the grid box parameters, and executing docking simulations. The docking results were saved in PDBQT format for further inspection. Validation and visualization of docking poses were carried out using PyMol, while 2D and 3D interaction analyses between ligands and receptor residues were examined using BIOVIA Discovery Studio.

### 3 Results and Discussion

This *in silico* research aims to identify and predict the pharmacokinetic and toxicity properties as well as antiviral potential active compounds in orange and mangosteen peel, which are known to exhibit various biological activities, in inhibiting SARS-CoV-2. Although not regularly consumed, orange and mangosteen peels are reported to contain bioactive compounds rich in flavonoids and polyphenols [2] [3]. This study tested 25 active compounds of orange and mangosteen peels, respectively, using ADME and toxicity analysis to predict the oral bioavailability of the compounds.

In developing a new drug, it is necessary to consider and investigate the aspects of absorption, distribution, metabolism, excretion, and toxicity before conducting *in vitro* and *in vivo* analysis. These five parameters can be predicted through an *in-silico* approach. Tables 1 and Tables 2 show the results of predictive analyses of pharmacokinetic and toxicity properties using the pkCSM online tool application. Intestinal absorption analysis and CaCO<sub>2</sub> permeability were used as parameters to predict the absorption rate of the tested compound. Absorption is the process of drug transfer from the site of extravascular administration into the circulatory system. Compounds with an Intestinal Absorption Human (%) value of >80% indicate that the compound is predicted to be well absorbed by the intestine [10]. Meanwhile, if the CaCO<sub>2</sub> permeability value is > 0.9, then the compound is predicted to have high intestinal mucosal permeability. In this research, 18 compounds from orange peel and 21 compounds from mangosteen peel were predicted to be well absorbed by the intestines (Table 1 and 2).

Volume of distribution at steady state (VD<sub>SS</sub>) and BBB / blood brain barrier are parameters used to characterize the distribution of the tested compound. Volume of distribution at steady state (VD<sub>SS</sub>) is the theoretical volume that a drug dose needs to be distributed evenly to give the same concentration as in blood plasma. [11] stated that when VD<sub>SS</sub> is lower than 0.71 L kg<sup>-1</sup> (log VD<sub>SS</sub> < -0.15), the volume of distribution is considered relatively low. When VD<sub>SS</sub> is higher than 2.81 L kg<sup>-1</sup> (log VD<sub>SS</sub> > 0.45), the distribution volume is considered relatively high. Therefore, the higher the VD<sub>SS</sub> log value, the more drug content is distributed to the tissues than plasma. A negative VD<sub>SS</sub> value indicates a low volume of distribution of the compound. In this research, 19 compounds from orange peel and 16 compounds from mangosteen peel had positive VD<sub>SS</sub> values. Meanwhile, BBB / blood-brain barrier is the ability of a drug to penetrate the blood-brain barrier. This can minimize side effects and toxicity, or increase the therapeutic effectiveness of drugs targeting

the brain. A compound is predicted to penetrate the blood–brain barrier (BBB) if it has a log BBB value higher than 0.3, and is considered poorly distributed to the brain if the log BBB value is less than  $-1$ .

Metabolism is a chemical process in which a drug is transformed into a metabolite within the body. The liver is an organ that is responsible for this process. Cytochrome P450 enzymes, mainly located in the liver and intestines, metabolize most drugs via oxidation. The two main subtypes of cytochrome P450 are CYP2D6 and CYP3A4. A CYP2D6 substrate is a compound metabolized by the enzyme, whereas a CYP2D6 inhibitor is a compound that can inhibit the enzyme's metabolic processes. A compound that exhibits dual potential as both a CYP2D6 inhibitor and a substrate is considered to promote unwanted drug-drug interactions [12]. In this study, all tested compounds had no potential as CYP2D6 inhibitors or substrates. Meanwhile, predicting the excretion process of the tested compound can be achieved by measuring the renal organic cation transporter 2 (OCT2) substrate. OCT2 is a renal uptake transporter that plays a crucial role in drug elimination through the kidneys. Renal OCT2 substrate is a compound that binds to OCT2. In this research, only 5-demethyltangeretin had the potential to be an OCT2 substrate. Previous studies reported that a drug with OCT2 substrate potential that interacts with other drugs identified as OCT2 inhibitors can potentially trigger undesirable effects, such as decreasing the excretion level of the drug (Müller et al., 2013). Therefore, we considered excluding compounds with OCT2 substrate potential. Meanwhile, LD50 is the concentration of a compound required to kill 50% of the population in a treatment group of animals (mg/kg body weight) [11]. Compounds in orange peel have an LD50 range of 2000-12,000 mg/kg BW, while compounds in mangosteen peel have an LD50 range of 500-3,850 mg/kg BW. According to [14], a compound is classified as slightly toxic as it has an LD50 value of 500–5,000 mg/kg, while a compound is practically non-toxic as it has an LD50 value of 5,000–15,000 mg/kg. Therefore, compounds in orange peel are relatively safer than compounds in mangosteen peel. Meanwhile, AMES toxicity predicts whether a compound has mutagenic and carcinogenic potential, while hepatotoxicity refers to compounds that can trigger liver damage [11]. Therefore, compounds with no AMES toxicity and hepatotoxicity potential are preferred

Based on the ADME-Toxicity parameters above [13], seven compounds from orange peel, namely Oxypeucedanin, Cadinene, Beta caryophyllene, Alpha phellandrene, Alpha terpinol, Alpha copaene, and Valencene demonstrated favorable pharmacokinetic properties, such as Intestinal Absorption Human (%) value of more than 80%, log VDss of more than 0, and exhibited no hepatotoxicity or mutagenic potential. Meanwhile, in mangosteen peel, seven compounds, namely Smeathxanthone A, Ledol, Garcinone B, Mangostenone A, Beta sitosterol, Tovophyllin B, and Anthocyanins, also showed good pharmacokinetic properties, including Intestinal Absorption Human (%) value of more than 80%, log VDss of more than 0, and exhibited no hepatotoxicity or mutagenic potential. Therefore, all of these compounds are considered non-toxic, with high intestinal permeability and distribution throughout the body's tissues. Each of these compounds was used as a ligand in molecular docking simulations at the receptor-binding domain (RBD) of the viral S1 glycoprotein.

Docking results of compounds derived from orange peel showed that all tested compounds, namely Oxypeucedanin, Cadinene, Beta caryophyllene, Alpha phellandrene, Alpha terpinol, Alpha copaene, and Valencene, had lower binding affinity compared to the positive control or native ligand, namely 2-acetamido-2-deoxy-beta-D-glucopyranose (-4.6 kcal/mol) (Table 3). The visualization of ligands and protein interaction is shown in Figure 1-14. This indicates that these compounds could bind the RBD site more strongly than the positive control. Meanwhile, Valencene interacted with the same amino acid residue as the positive control, namely GLY339. The similarity of amino acid residues bound to the positive

**Table 1.** Prediction of analysis ADME and Toxicity for Active Compounds

No	Active compound	Absorption		Distribution		Metabolism		Excretion		Toxicity		
		Intestinal Absorption Human (%)	Permeability CaCO <sub>2</sub> (10 <sup>-6</sup> cm/s)	VDSS (Log L/kg)	Permeability BBB (Log BB)	CYP2D6 substrate	CYP2D6 inhibitor	Renal substrate	LD <sub>50</sub> (mg/kg)	AMES Toxicity	Hepatotoxicity	
1	<b>2-acetamido-2-deoxy-beta-D-glucopyranose (Native ligand)</b>	<b>31.963</b>	<b>-0.219</b>	<b>0.041</b>	<b>-0.618</b>	<b>No</b>	<b>No</b>	<b>No</b>	<b>No</b>	<b>5000</b>	<b>No</b>	<b>No</b>
2	Auraptene	95.416	1.634	0.491	0.129	No	No	No	No	2274	No	Yes
3	Bergamotin	95.727	1.448	0.792	0.085	No	Yes	No	No	2321	Yes	No
4	Imperatorin	97.755	1.383	0.147	0.176	No	No	No	No	2200	Yes	No
5	Heraclenin	98.680	0.830	-0.028	0.113	No	No	No	No	2290	No	No
6	Oxypeucedanin	98.571	1.033	0.104	0.070	No	No	No	No	2295	No	No
7	5-demethylangeretin	96.145	1.148	-0.217	-0.909	No	No	Yes	Yes	2344	No	No
8	Cadinene	96.179	1.421	0.665	0.806	No	No	No	No	5000	No	No
9	Beta carophyllene	94.845	1.423	0.652	0.733	No	No	No	No	5300	No	No
10	Alpha phellandrene	96.548	1.414	0.408	0.761	No	No	No	No	5700	No	No
11	Alpha terpinol	94.183	1.489	0.207	0.305	No	No	No	No	2830	No	No
12	Flavone	97.386	1.263	0.129	0.165	No	No	No	No	2500	Yes	No
13	Alpha copaene	96.221	1.374	0.806	0.887	No	No	No	No	3700	No	No
14	Hesperetin	70.277	0.294	0.746	-0.719	No	No	No	No	2000	No	No
15	p-hydroxybenzoic acid	83.961	1.151	-1.557	-0.334	No	No	No	No	2200	No	No
16	Chlorogenic acid	36.377	-0.840	0.582	-0.141	No	No	No	No	5000	No	No
17	Valencene	94.127	1.401	0.686	0.776	No	No	No	No	5000	No	No
18	Narirutin	36.625	0.521	1.295	-1.594	No	No	No	No	2300	No	No
19	Hesperidin	31.481	0.505	0.996	-1.715	No	No	No	No	12000	No	No
20	Sinensetin	98.578	1.233	-0.188	-1.008	No	No	No	No	5000	No	No
21	Epicatechin	68.829	-0.283	1.027	-1.054	No	No	No	No	10000	No	No
22	Catechine	68.829	-0.283	1.027	-1.054	No	No	No	No	10000	No	No
23	Naringenin	91.310	1.029	-0.015	-0.578	No	No	No	No	2000	No	No
24	Nobiletin	98.921	1.306	-0.281	-1.254	No	No	No	No	5000	No	No
25	Tangeretin	98.478	1.245	-0.226	-1.026	No	No	No	No	5000	No	No
26	Naringin	25.796	-0.658	0.619	-1.600	No	No	No	No	2300	No	No

**Table 2.** Prediction of analysis ADME and Toxicity for Active Compounds in Mangosteen Peel

No	Active compound	Absorption		Distribution		Metabolism		Excretion		Toxicity		
		Intestinal Absorption Human (%)	Permeability CaCO <sub>2</sub> (10 <sup>-5</sup> cm/s)	VDSS (Log L/kg)	Permeability BBB (Log BB)	CYP2D6 substrate	CYP2D6 inhibitor	Renal substrate	OCT2 substrate	LD <sub>50</sub> (mg/kg)	AMES Toxicity	Hepatotoxicity
1	<b>2-acetamido2-deoxy-beta-D-glucopyranose (Native ligand)</b>	<b>31.963</b>	<b>-0.219</b>	<b>0.041</b>	<b>-0.618</b>	<b>No</b>	<b>No</b>	<b>No</b>	<b>No</b>	<b>5000</b>	<b>No</b>	<b>No</b>
2	Alpha mangostin	93.647	-0.048	-0.282	-1.075	No	No	No	No	1500	Yes	No
3	Beta mangostin	91.635	1.218	-0.319	-0.261	No	No	No	No	1500	Yes	No
4	Gartanin	82.370	0.252	-0.309	-1.224	No	No	No	No	1500	No	No
5	Xanthone	98.514	1.224	0.26	0.149	No	No	No	No	1680	Yes	No
6	Gamma mangostin	89.405	-0.165	-0.359	-1.147	No	No	No	No	3200	No	No
7	Smeathxanthone A	88.465	0.029	0.429	-0.986	No	No	No	No	500	No	No
8	Tovophyllin A	99.653	0.289	-0.052	-1.044	No	No	No	No	2500	Yes	Yes
9	Caffeic acid	69.407	0.634	-1.098	-0.608	No	No	No	No	2980	No	No
10	Ledol	92.814	1.483	0.556	0.632	No	No	No	No	2000	No	No
11	Thwaitesixanthone	96.286	1.157	0.532	-0.358	No	No	No	No	3850	Yes	Yes
12	Garcinone B	100	0.381	0.483	-1.022	No	No	No	No	550	No	No
13	Mangostenone A	94.051	0.708	0.764	-0.165	No	No	No	No	3850	No	No
14	Beta sitosterol	94.464	1.201	0.193	0.781	No	No	No	No	890	No	No
15	Gambogic acid	97.871	0.742	-0.622	-0.423	No	No	No	No	500	No	No
16	Calabaxanthone	95.899	0.576	0.519	-0.418	No	No	No	No	2500	Yes	No
17	Garcinone E	90.397	-0.234	-0.792	-1.137	No	No	No	No	1500	Yes	Yes
18	Taxifolin	64.709	0.924	1.638	-0.725	No	No	No	No	2000	No	No
19	Oleanolic acid	99.931	1.170	-1.085	-0.14	No	No	No	No	2000	No	Yes
20	Tovophyllin B	92.468	1.178	0.670	-0.300	No	No	No	No	1050	No	Yes
21	Epicatechin	68.829	-0.283	1.027	-1.054	No	No	No	No	2.428	No	No
22	Catechine	68.829	-0.283	1.027	-1.054	No	No	No	No	2.428	No	No
23	Anthocyanins	96.182	1.631	0.240	0.454	No	No	No	No	1.848	No	No
24	Proanthocyanidins	71.723	0.188	-0.307	-1.682	No	No	No	No	2.483	No	No
25	Hexadecanoic acid	92.004	1.558	-0.543	-0.111	No	No	No	No	1.440	No	No
26	Mangostanol	87.526	0.534	0.564	-1.243	No	No	No	No	2.001	Yes	No

**Table 3.** Docking motive of Native Ligand and test compound

No.	Orange Peel			No	Mangosteen Peel		
	Compound	$\Delta G$ (kcal/mol)	Interaction with amino acid residues		Compound	( $\Delta G$ ) (kcal/mol)	Interaction with amino acid residues
1.	2-acetamido-2-deoxy-beta-D-glucopyranose (Native ligand)	-4,6	- ASN343, GLY339	1.	2-acetamido-2-deoxy-beta-D-glucopyranose (Native ligand)	-4,6	- ASN343, GLY339
2	Oxypeucedamin	-6,7	- ARG454, SER469, GLU471, GLN474, GLU471, ARG457	2	Smeathxanthone A	-6,7	- ARG346, ASN450, TYR351, SER349, VAL341, ALA344, LYS356, ALA348
3	Cadinene	-5,7	- ALA348, SER399, PHE347, ALA348, VAL341, ALA344, LYS356	3	Ledol	-6,5	- THR430, PRO426, PHE464
4	Beta caryophyllene	-6,2	- PHE464	4	Garcinone B	-6,9	- SER373, TRP436, LEU368
5	Alpha phellandrene	-5,1	- TYR473	5	Mangostenone A	-7,5	- SER373, SER371, TRP436, VAL367, PHE374
6	Alpha terpinol	-5,3	- SER469, GLU471, TYR473	6	Beta sitosterol	-6,5	- THR430, PHE515, PHE464
7	Alpha copaene	-5,7	- ARG454, SER469, LYS458, TYR473	7	Tovophyllin B	-7,2	- SER373, PHE374, TRP436
8	Valencene	-5,7	- GLY339, PHE374, TRP436	8	Anthocyanins	-6,4	- LEU368, PHE374, TRP436

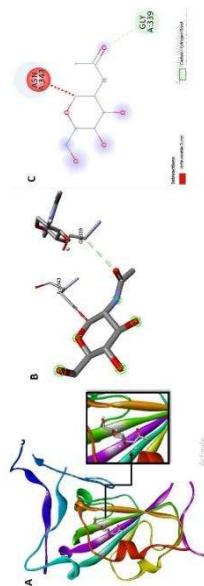


**Figure 1.** (A) Simulation *molecular docking* protein (PDB ID : 7BZ5) with 2-acetamido-2-deoxy-beta-D-glucopyranose (Native ligand) ; (B) interaction 3D structure; and (C) 2D

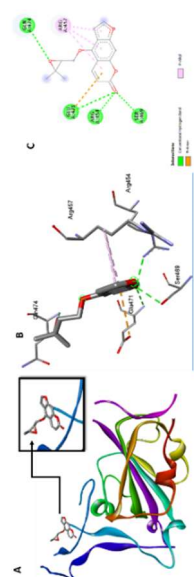


**Figure 2.** (A) Simulation *molecular docking* protein (PDB ID : 7BZ5) with Oxypeucedanin; (b) interaction 3D structure; and (C) 2D

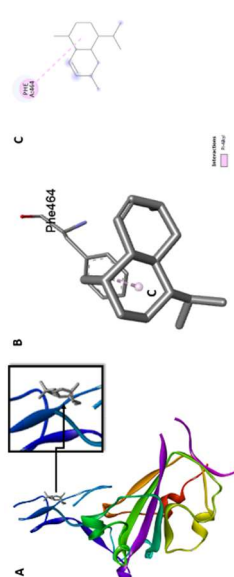


**Figure 3.** (A) Simulation *molecular docking* protein (PDB ID : 7BZ5) with Beta caryophyllene; (b) interaction 3D structure; and (C) 2D

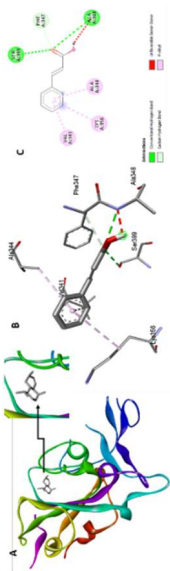


**Figure 4.** (A) Simulation *molecular docking* protein (PDB ID : 7BZ5) with Cadimene; (b) interaction 3D structure; and (C) 2D

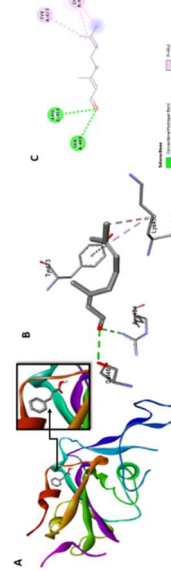


**Figure 5.** (A) Simulation *molecular docking* protein (PDB ID : 7BZ5) with Alpha copaene; (b) interaction 3D structure; and (C) 2D

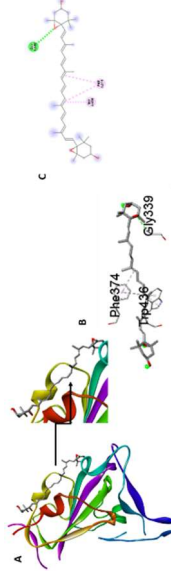


**Figure 6.** (A) Simulation *molecular docking* protein (PDB ID : 7BZ5) with Valencene; (b) interaction 3D structure; and (C) 2D

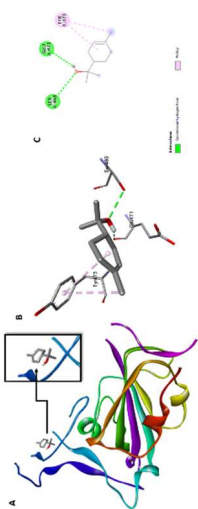


**Figure 7.** (A) Simulation *molecular docking* protein (PDB ID : 7BZ5) with Alpha terpinol; (a) Complexs protein-ligan; (b) interaction 3D structure; and (C) 2D

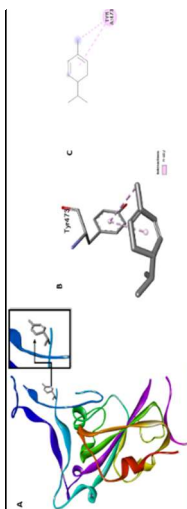


**Figure 8.** (A) Simulation *molecular docking* protein (PDB ID : 7BZ5) with Alpha phellandrene; (a) Complexs protein-ligan; (b) interaction 3D structure; and (C) 2D

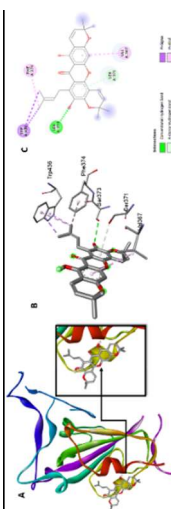
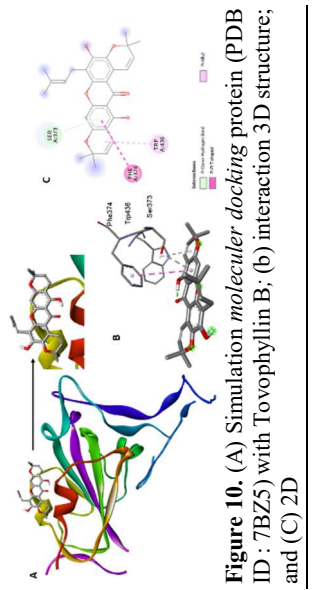
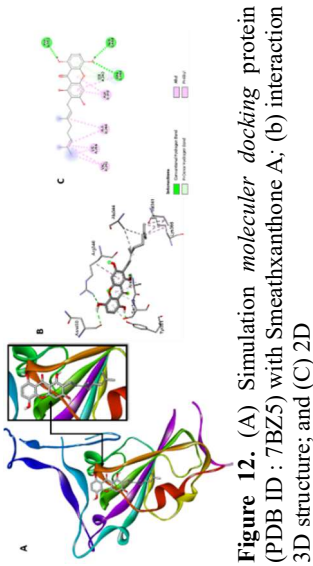
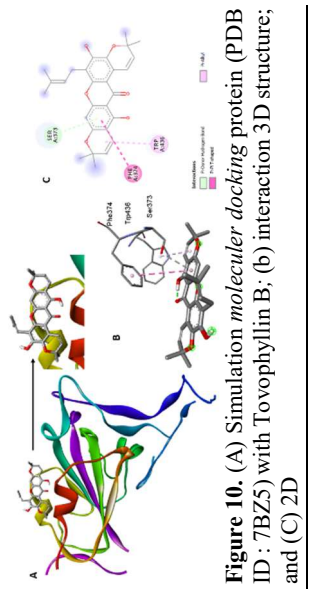
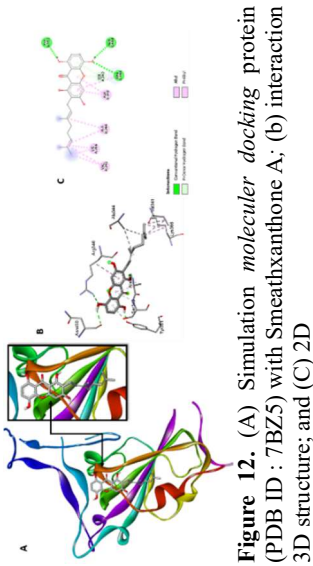


**Figure 9.** (A) Simulation *molecular docking* protein (PDB ID : 7BZ5) with Mangostenone A; (b) interaction 3D structure; and (C) 2D



Control in the docking study may indicate a similar mechanism in inhibiting the RBD site with the positive control. Alpha phellandrene, Alpha terpinol, and Alpha copaene could bind to one of the amino acid residues involved in hACE2-RBD binding [10]. The interaction of these compounds with the key residues indicates the possibility of their inhibitory activity on the interaction between RBD and ACE2. In addition, Cadinene and Valencene interacted with several amino acid residues, including VAL341, ALA344, PHE374, and TRP436, constituents of the RBD pocket that can be potential allosteric targets in inhibiting the RBD [15]. Therefore, these compounds are predicted to inhibit the virus allosterically. However, this molecular docking analysis requires further study to validate these results.

Docking results of compounds derived from mangosteen peel showed that all compounds, namely Smeathxanthone A, Ledol, Garcinone B, Mangostenon A, Beta sitosterol, Tovophyllin B, and Anthocyanins, had lower binding affinity compared to the positive control or native ligand, namely 2-acetamido-2-deoxy-beta-D-glucopyranose (-4.6 kcal/mol). This indicates that these compounds could bind protein sites more strongly than the positive control. Meanwhile, no compounds bound the same amino acid residues as the positive control. However, some compounds, such as Smeathxanthone A, Garcinone B, Mangostenon A, Tovophyllin B, and Anthocyanins, bound VAL341, ALA344, TRP436, LEU368, VAL367, and PHE374, residues that are parts of a potential allosteric pocket on the RBD [15]. This molecular docking analysis requires further experiments to confirm these results.

## 4 Conclusions

This study concluded that ADME values, toxicity, and binding affinity tests indicated that several key compounds in orange and mangosteen peels have the potential to be developed as oral drugs that can inhibit the SARS-CoV-2 virus through disrupting the RBD and ACE2 interactions and inhibition at allosteric sites. The results obtained in this study can be continued into molecular dynamics simulation analysis, *in vitro*, and *in vivo* to explore the inhibition of other types of viruses.

## Acknowledgment

We are thankful to Universitas Islam Malang, which has provided research funds through the 2020 University Institutional Grant (HiMa) scheme.

## References

1. MISM. Radzuan, M. Karuppanan, Adverse events associated with antivirals for COVID-19: An analysis based on the FDA Adverse Event Reporting System (FAERS). *Current Drug Safety*. **20**, 4 (2025).  
<https://doi.org/10.2174/0115748863334598241203073907>
2. C. Bi, H. Xu, J. Yu, Z. Ding, Z. Liu, Botanical characteristics, chemical components, biological activity, and potential applications of mangosteen. *PeerJ* **11**, e15329 (2023).  
<https://doi.org/10.7717/peerj.15329>
3. RK. Saini, A. Ranjit, K. Sharma, P. Prasad, X. Shang, KGM. Gowda, YS. Keum, Bioactive Compounds of Citrus Fruits: A Review of Composition and Health Benefits of Carotenoids, Flavonoids, Limonoids, and Terpenes. *Antioxidants (Basel)*. **11**, 2 (2022). doi: [10.3390/antiox11020239](https://doi.org/10.3390/antiox11020239).

4. A. Ahmadi, P. Hassandarvish, R. Lani, P. Yadollahi, A. Jokar, SA. Bakar, K. Zandi, Inhibition of chikungunya virus replication by hesperetin and naringenin. *RSC Advances*, **6**, 73 (2016). <https://doi.org/10.1039/c6ra16640g>
5. L. Gao, M. Zu, S. Wu, AL. Liu, GH. Du, 3D QSAR and docking study of flavone derivatives as potent inhibitors of influenza H1N1 virus neuraminidase. *Bioorganic and Medicinal Chemistry Letters*, **21**, 19 (2011). <https://doi.org/10.1016/j.bmcl.2011.07.071>
6. Mohammadi Zonouz A, Ghasemzadeh Rahbardar M, Hosseinzadeh H. Antidotal and protective effects of mangosteen (*Garcinia mangostana*) against natural and chemical toxicities: A review. *Iran J Basic Med Sci*. **26**, 5 (2023). <https://doi.org/10.22038/IJBMS.2023.66900.14674>
7. M. Hoffmann, H. Kleine-Weber, S. Pöhlmann, A multibasic cleavage site in the spike protein of SARS-CoV-2 is essential for infection of human lung cells. *Molecular Cell*, **78**, 4 (2020). <https://doi.org/10.1016/j.molcel.2020.04.022>
8. A. Milewska, A. Kula-Paczur, J. Wadas, A. Suder, A. Szczepański, A. Dąbrowska, K. Owczarek, A. Marcello, M. Ochman, T. Staćel, Z. Rajfur, M. Sanak, P. Labaj, W. Branicki, K. Pyrc, Replication of severe acute respiratory syndrome coronavirus 2 in human respiratory epithelium. *Journal of Virology*. **94**, 15 (2020). <https://doi.org/10.1128/JVI.00957-20>
9. T. Mir, T. Almas, J. Kaur, M. Faisaluddin, D. Song, W. Ullah, S. Mamtani, H. Rauf, S. Yadav, S. Latchana, NM. Michaelson, M. Connerney, Y. Sattar, Coronavirus disease 2019 (COVID-19): Multisystem review of pathophysiology. *Annals of Medicine and Surgery (London)*. **69**, 102745. (2021). <https://doi.org/10.1016/j.amsu.2021.102745>
10. Y. Wu, F. Wang, C. Shen, W. Peng, D. Li, C. Zhao, Z. Li, S. Li, Y. Bi, Y. Yang, Y. Gong, H. Xiao, Z. Fan, S. Tan, G. Wu, W. Tan, X. Lu, C. Fan, Q. Wang, Y. Liu, C. Zhang, J. Qi, GF. Gao, F. Gao, L. Liu, A noncompeting pair of human neutralizing antibodies block COVID-19 virus binding to its receptor ACE2. *Science*, **368**, 1274-1278. (2020). doi: [10.1126/science.abc2241](https://doi.org/10.1126/science.abc2241).
11. DEV. Pires TL. Blundell DB. Ascher, pkCSM: Predicting Small Molecule Pharmacokinetic and Toxicity Properties Using GraphBased Signatures. *Journal of Medicinal Chemistry*, **58**, 9 (2015). <https://doi.org/10.1021/acs.jmedchem.5b00104>
12. Y. Wei, L. Palazzolo, O. Ben Mariem, D. Bianchi, T. Laurenzi, U. Guerrini, I. Eberini, Investigation of in silico studies for cytochrome P450 isoforms specificity. *Computational and Structural Biotechnology Journal*. **23**, 3090–3103 (2024). <https://doi.org/10.1016/j.csbj.2024.08.002>
13. TA. Loomis and AW. Hayes, Clinical toxicology. In TA. Loomis and A.W. Hayes (Eds.), *Loomis's essentials of toxicology*. (Academic Press, 1996). <https://doi.org/10.1016/B978-012455625-6/50014-3>
14. X. Zhang, J-P. Yun, Y-N. Yang, Z-M. Feng, J-S. Jiang, X. Yuan, W. Liu, P-C. Zhang, Synthesis of 4-thiosubstituted flavan derivatives and their hypoglycemic activities. *Fitoterapia*, **161**, 105255 (2022). <https://doi.org/10.1016/j.fitote.2022.105255>
15. G. Gupta, G. Verkhivker, Exploring binding pockets in the conformational states of the SARS-CoV-2 spike trimers for the screening of allosteric inhibitors using molecular simulations and ensemble-based ligand docking. *International Journal of Molecular Sciences*, **25**, 9 (2024). <https://doi.org/10.3390/ijms25094955>